Analytical Methods

ROYAL SOCIETY OF CHEMISTRY

PAPER

View Article Online
View Journal | View Issue

Cite this: *Anal. Methods*, 2025, **17**, 1389

A rhodamine-conjugated fluorescent and colorimetric receptor for the detection of Cu^{2+} ions: environmental utility and smartphone integration†

Karuppaiyan Kaviya, ‡[ab] Ramar Rajamanikandan, *[c] Madhappan Santhamoorthy, ‡[de] Mohammad Abul Farah[f] and Kailasam Saravana Mani *[ab]

A new rhodamine based turn on florescent probe (*Z*)-3′,6′-bis(ethylamino)-2-(((6-methoxy-2-oxo-1,2-dihydroquinolin-3-yl)methylene)amino)-2′,7′-dimethylspiro[isoindoline-1,9′-xanthen]-3-one (**RME**) was efficiently synthesized through a simple condensation reaction of 2-amino-3′,6′-bis(ethylamino)-2′,7′-dimethylspiro[isoindoline-1,9′-xanthen]-3-one and 6-methoxy-2-oxo-1,2-dihydroquinoline-3-carbaldehyde. The receptor **RME** is highly non-fluorescent and when copper ions (Cu^{2+} ions) are added in DMF/water (1 : 2, v/v) medium, the receptor **RME** exhibits a specific "turn-on" colorimetric and fluorometric response. Moreover, **RME** binding with Cu^{2+} ions produced a remarkable color variation that was perceptible to the human eye, changing from colorless to pink. The binding stoichiometry was 1 : 1, confirmed through theoretical DFT, Job's plot, and mass spectral analysis. **RME** showed good sensing capability for Cu^{2+} ions, with LOD values of 11.25 nM for ratiometric colorimetry, 1.42 nM for fluorometry, and 107 nM for smartphone-based detection. These LOD values are significantly lower than WHO's acceptable threshold of 2 μM. Additionally, developing portable techniques based on paper-based test strips and smartphone assistance allowed for qualitative and quantitative detection of Cu^{2+} ions. These portable and economical methods eliminate the need for expensive laboratory apparatus, enabling precise and affordable on-site assessments. In addition, the developed sensing protocol for the detection of Cu^{2+} ions was extended to real water samples such as tap, dam, and drinking water samples. These results demonstrated the effectiveness of **RME** in detecting Cu^{2+} ions in complex matrices, making it a promising tool for environmental monitoring and water quality assessment.

Received 22nd October 2024
Accepted 28th December 2024

DOI: 10.1039/d4ay01925c

rsc.li/methods

1. Introduction

Industrial chemical waste streams often contain hazardous waterborne pollutants, including heavy metal ions, bacteria, viruses, and organic solvents. Because of their incapacity to break down in biological systems, heavy metals are among the substances that pose the greatest hazard to all living things, including humans. Heavy metals can therefore accumulate in tissues and cause a variety of health concerns.[1,2] It is now urgently necessary to purify contaminated water due to the increasing lack of clean water. After iron and zinc, copper is the third most abundant essential metal in the human body, playing a critical role as a nutrient in various biological systems. However, at elevated levels, it becomes toxic, making its detection crucial in chemical, biological, and environmental studies. Furthermore, plants, animals, and humans all require Cu^{2+} ions as a trace element.[3] However, the absence or excess copper amounts may result in diseases like kidney and liver damage and[4] neurotoxicity[5] and also cause Wilson's disease, gastrointestinal disorders, hypoglycemia, liver disease, and dyslexia in babies.[6–10] Owing to the concentration-dependent nature of Cu^{2+} ions, guidelines have been released by the World Health Organization to guarantee that the concentration of Cu^{2+} ions in drinking water is kept below 2 ppm.[11] Anthropogenic activities

[a]*Department of Chemistry, Karpagam Academy of Higher Education, Coimbatore, Tamil Nadu, India. E-mail: chemsaran.mani@gmail.com*

[b]*Centre for Material Chemistry, Karpagam Academy of Higher Education, Coimbatore, Tamil Nadu, India*

[c]*Department of Physics, Gachon University, Seongnam-si, 13120, Republic of Korea. E-mail: chemistrmkd@gmail.com*

[d]*Department of Physiology, Saveetha Dental College and Hospitals, Saveetha Institute of Medical and Technical Science (SIMATS), Saveetha University, Chennai, 600077, India*

[e]*School of Chemical Engineering, Yeungnam University, Gyeongsan 38544, Republic of Korea*

[f]*Department of Zoology, College of Science, King Saud University, Riyadh 11451, Saudi Arabia*

† Electronic supplementary information (ESI) available: The NMR spectra, mass spectra, DFT theoretical data, and additional data. See DOI: https://doi.org/10.1039/d4ay01925c

‡ These authors contributed equally to this work.

such as mining, industrial processes, and agricultural practices emit Cu^{2+} ions into the air, soil, and water, increasing their concentration in our surroundings.[12–14] Cu^{2+} ions are one of the main elements required for the normal functioning of living organisms. They catalyze reactions and help transfer electrons within DNA and RNA.[15–19] It is extremely desirable and in great demand to counteract this concentration-dependent variable behavior of Cu^{2+} ions with something simple, selective, sensitive, and especially below the allowable limit.

Until now, Cu^{2+} ions had only been applied in a few widely used, very expensive instrumental methods, like atomic absorption spectroscopy (AAS),[20] inductively coupled plasma atomic emission spectroscopy (ICP-AES),[21] potentiometry,[22] anodic stripping voltammetry,[23] spectrophotometry, and spectrofluorimetry.[24] Of the methods mentioned above, spectrophotometric and fluorescence chemosensors have garnered the most interest from research groups working in a variety of fields.[25] For example, appropriate chemosensors for detecting heavy metal ions are critical due to the direct benefits applicable to essential areas such as the environment, industry, biology, and human health. Optical chemosensors are popular due to their great sensitivity, selectivity, and ease of fabrication. They also display metal-ion-specific fluorescence. In the past few years, fluorescent compounds with heavy metal detection capabilities have emerged as the most fascinating field of study.[26] Scientists and researchers primarily use colorimetric or fluorescence methods to determine the presence of heavy metal ions in their work; however, the latter have more affordable and rapid procedures that are easier to apply. In analytical chemistry, creating innovative Cu^{2+} sensors with less expensive equipment has become popular.[27] Because of its quick response time, good spectral resolution, and simple sample preparation, fluorescence is one of the most popular technologies.[28] It is noted that multiple events demonstrate how the coordination of Cu^{2+} affects the photophysical behavior of the receptor. In particular, the main reason why Cu^{2+} can be detected *via* CHEQ or CHEF methods is electronic changes based on charge transfer from the ligand to metal (LMCT – ligand-to-metal charge transfer).[29] Turn-on fluorescent sensors are favored over turn-off fluorescein-based chemosensors because low sensitivity and turn-off detection are caused by background fluorescence.[30]

Rhodamine is the fluorophore moiety of a variety of fluorescent probes that have the most potential in creating fluorescence sensors for ions and molecules. Rhodamine conjugates exhibit a visual color shift in the presence of analytes, which allows the analytes to be quickly detected.[31–34] This "off–on" process of accuracy and efficiency of rhodamine makes it feasible for researchers to develop a large number of rhodamine derivatives for rapid recognition and visual determination of metal ions with the naked eye.[35,36] This occurs since rhodamine and rhodamine derivatives have a spirocyclic ring, which results in ring opening, causing a notable color change as well as absorbance or fluorescence alterations.[37,38] Rhodamine dyes with improved emission maxima, visible excitation, photostability,[39] and excellent spectroscopic properties are used as biomarkers, in industrial coloring, and as sensing probes. The rhodamine derivatives we obtained which had an open spirolactam ring exhibit a bright pink color and luminous emission due to metal ion chelation.[40] In particular, a chemosensor that possesses twin signalling capabilities that is, one that can both generate a discernible shift and increase fluorescence emission will achieve the detection objective. While the majority of described receptors show fluorescence quenching upon interaction with copper ions, only a limited number of sensors for Cu^{2+} have been shown to exhibit increased fluorescence.[41–43] The successful utilization of our compound's fluorescence in response to Cu^{2+} ions was effectively applied for live cell imaging.[44]

Herein, we describe a rhodamine-based chemosensor **RME** that operates in the longer wavelength range with excitation and emission both as a colorimetric and a turn-on fluorescence chemosensor upon binding Cu(II) ions in the DMF/water medium. The sensing mechanism has been examined by systematic spectral and theoretical studies. The notable colorimetric changes observed in the current work were further extended to smartphone-based detection of Cu^{2+} ions. As expected, **RME** can specifically recognize and quantify Cu^{2+} ions from potentially interfering metal ions, with the lowest detection limit as low as 11.25 nM. Furthermore, photometric titrations verified the complexation ratio of 1 : 1 as per JOB's working diagram and the fluorescence enhancement of **RME** by Cu^{2+} ions. A reversible Cu^{2+} detection device was developed with the aid of EDTA, and an implication logic gate was also constructed for Cu^{2+} detection. Finally, **RME** was effectively applied to determine Cu^{2+} ions in real water samples and paper strip applications.

2. Experimental section

2.1. Materials and instrumentation

All the reagents and solvents were purchased from commercial sources. Rhodamine 6G and hydrazine hydrate 80% were sourced from Sigma Aldrich. FT IR spectra were measured using the BRUKER Alpha II model in ATR mode. ^{1}H and ^{13}C NMR spectra were recorded on a Bruker Avance Neo (400 MHz) in DMSO-d_6 solvent. Alumina-coated F254 Merck plates were used in TLC to monitor the reaction progress. ESI-MS spectra were recorded on a Thermo Scientific High-Resolution Magnetic Sector MS DFS by the positive ion electrospray ionization (ESI) method. UV-visible absorbance spectra were recorded using a JASCO V-750 spectrophotometer. Fluorescence spectrum experiments are conducted using a Horiba Fluoromax Plus spectrofluorometer. Tap and drinking water samples were taken from our university campus (Karpagam Academy of Higher Education) and dam water samples were collected from Siruvani Dam, Coimbatore. Without any pretreatment, collected water samples were utilized for real sample investigations.

2.2. Synthesis of RME

The synthesis of 6-methoxy-2-oxo-1,2-dihydroquinoline-3-carbaldehyde was carried out by employing the Vilsmeier–Haack formylation procedure by using a mixture of *p*-anisidine

and acetic anhydride to get *N*-(4-methoxyphenyl)acetamide which undergoes formylation to afford 2-chloro-6-methoxy quinoline-3-carbaldehyde; furthermore, this aldehyde was hydrolyzed to get 6-methoxy-2-oxo-1,2-dihydroquinoline-3-carbaldehyde by following the previous work.[45] The synthesis of Rhodamine 6G hydrazide was carried out by using Rhodamine 6G and hydrazine hydrate 80% in ethanol medium. The reaction mixture was stirred and refluxed at 90 °C for 6 h. The resulting precipitate was filtered, washed with distilled water, and left to dry. The crude product was crystallized with ethanol. The rhodamine 6G hydrazide was obtained as a pink solid.[46]

The probe **RME** was synthesized by adding an equimolar mixture of synthesized 6-methoxy-2-oxo-1,2-dihydroquinoline-3-carbaldehyde (0.09 g, 1 mmol) and rhodamine 6G hydrazide (0.2 g, 1 mmol) in 10 mL of ethanol, and the reaction mixture was allowed to reflux at 90 °C in an oil bath. The reaction process was monitored by TLC, and the obtained precipitate was filtered and then completely washed with cold ethanol. The product was vacuum dried and taken for further steps without any purification.

2.2.1 (*Z*)-3′,6′-Bis(ethylamino)-2-(((6-methoxy-2-oxo-1,2-dihydroquinolin-3-yl)methylene)amino)-2′,7′-dimethylspiro[isoindoline-1,9′-xanthen]-3-one (RME). Yellow powder; yield: 80%; MP 320–325 °C; FTIR ν (cm^{-1}): 1711 (C═O), 2965 (–NH), 1646 (CH═N); ^{1}H NMR (400 MHz, DMSO-d_6) δppm: 11.74 (s, 1H), 8.61 (s, 1H), 8.13 (s, 1H), 7.93 (d, J = 4.0 Hz, 1H), 7.58–7.53 (m, 2H), 7.26–7.20 (m, 2H), 7.13 (s, 1H), 6.99 (d, J = 4.0 Hz, 1H), 6.35 (s, 2H), 6.22 (s, 2H), 5.06 (s, 2H), 4.36 (s, 1H), 3.76 (s, 3H), 3.15 (t, J = 8.0 Hz, 4H), 1.86 (s, 6H), 1.23 (t, J = 8.0 Hz, 6H); ^{13}C NMR (100.1 MHz) δppm: 164.63, 160.68, 154.82, 152.87, 151.14, 148.24, 141.08, 134.46, 134.16, 134.12, 129.02, 127.94, 126.96, 126.42, 124.02, 123.58, 121.27, 119.78, 118.72, 116.81, 110.21, 104.97, 96.54, 65.66, 55.89, 19.02, 17.46, 14.63, 37.94. MS (ESI – M + Na) m/z 636.6. Anal. calcd For $C_{37}H_{35}N_5O_4$; C, 72.41; H, 5.75; N, 11.41; Found; C, 72.45; H, 5.71; N, 11.42.

2.3. General procedure for absorption and fluorescence measurements

RME stock solution (10 mM) was prepared by adding 6.4 mg in 10 mL of DMF solution and the stock solution (1 mM) of Cu^{2+} ions was prepared in double distilled water. For photometric titration experiments, a cuvette was filled with 10 μM **RME** dissolved in 2.5 mL of DMF/water (1 : 3, v/v). Subsequently, appropriate amounts of Cu^{2+} stock solution were blended with the reaction mixture and shaken well. After a 2 min incubation period, the UV-vis absorbance spectra were recorded in the range of 600 nm to 200 nm. A similar protocol was followed for fluorescence spectral investigations. The excitation wavelength for the fluorescence spectra was set at 415 nm, and spectrum analysis was carried out after 2 min with a 2/2 nm slit emission/excitation slid width. Absorbance/emission spectrum investigations were used in a photometric titration based technique, and specificity measurements were carried out in place of Cu^{2+} ions and other potentially interfering metal ions mixed with the reaction mixture. All the sensing-related measurements were performed a minimum of three times.

2.4. Smartphone assisted Cu^{2+} recognition

To identify Cu^{2+} in DMF–H_2O (1 : 3 v/v) solution, a smartphone-based color assist application (color Grap) was applied to digitalize the color shift of **RME** with Cu^{2+} that can be seen with the naked eye. In a glass tube, different quantities of Cu^{2+} ions were mixed in **RME** (10 μM) in a DMF/water medium. Color variations were captured on the back camera of a Vivo V23 Pro smartphone. Lastly, the Color Grab app, a freely available mobile application, digitalized the red, green, and blue (RGB) values of the photos.

2.5. Paper strip application

The first identical-size Whatman filter paper was developed to create the paper-based test strips. The Whatman filter paper was soaked in an **RME**-dissolved DMF/water stock solution to make **RME** sensor test strips and dried in air. Subsequently, **RME**-coated paper test strips were spiked into standard solutions of Cu^{2+} ions and dried in air. Finally, colorimetric images of the paper-based test strips were taken using a Vivo V23 Pro (108 MP camera resolution) under ambient conditions (without flash).

3. Results and discussion

3.1. Design and synthesis of the probe

The synthesis of the fluorescent receptor **RME** was explored and is outlined in Scheme 1 *via* the well-known Schiff-base condensation reaction of compound 6-methoxy-2-oxo-1,2-dihydroquinoline-3-carbaldehyde and rhodamine 6G hydrazide under reflux conditions at 90 °C in ethanol medium. The rhodamine 6G hydrazide and the compound 6-methoxy-2-oxo-1,2-dihydroquinoline-3-carbaldehyde were synthesized by using the previously described technique.[45,46] The structure of the synthesized receptor, **RME** was attested through spectroscopic techniques like FTIR, ^{1}H and ^{13}C NMR, and ESI-MS spectral analysis.

In the IR spectrum of probe **RME**, the characteristic peaks at 1711 cm^{-1}, 2965 cm^{-1}, and 1646 cm^{-1} were attributed to –C═O, –NH –C═N, and functional groups respectively (Fig. S1†) The ^{1}H NMR spectrum of the receptor RME (Fig. S2†), the –NH proton appearing at δ 11.78 ppm as a singlet corresponds to the quinoline core, OCH_3 appeared at δ 3.76 ppm as a singlet, azomethine proton CH═N appeared at δ 8.6 ppm as a singlet, two –NH protons present in the rhodamine core appeared at δ 6.22 ppm as singlets, $-CH_2$ protons in the ethyl group appeared as a triplet at δ 3.15 ppm and $-CH_3$ protons in the ethyl group appeared as a triplet at δ 1.25 ppm of the rhodamine core. In the ^{13}C NMR spectrum (Fig. S3†), the peak at δ 56.5 ppm was due to OCH_3 and the peak at δ 164.3 ppm was due to –NHC═O in the quinoline core. The –C═O carbon in the indole core appeared at δ 160.6 ppm and the two $-CH_3$ carbons appeared at δ 14.6 ppm and $-CH_2CH_3$ carbons appeared at δ 37.9, 17.4 and 19.0 ppm respectively. Furthermore, the molecular ion peak at m/z 614.6 $(M + H)^+$ (ESI-MS) (Fig. S4†) confirms the structure of **RME** as (*Z*)-3′,6′-bis(ethylamino)-2-(((6-methoxy-2-oxo-1,2-dihydroquinolin-3-yl)methylene)amino)-2′,7′-dimethylspiro[isoindoline-1,9′-xanthen]-3-one.

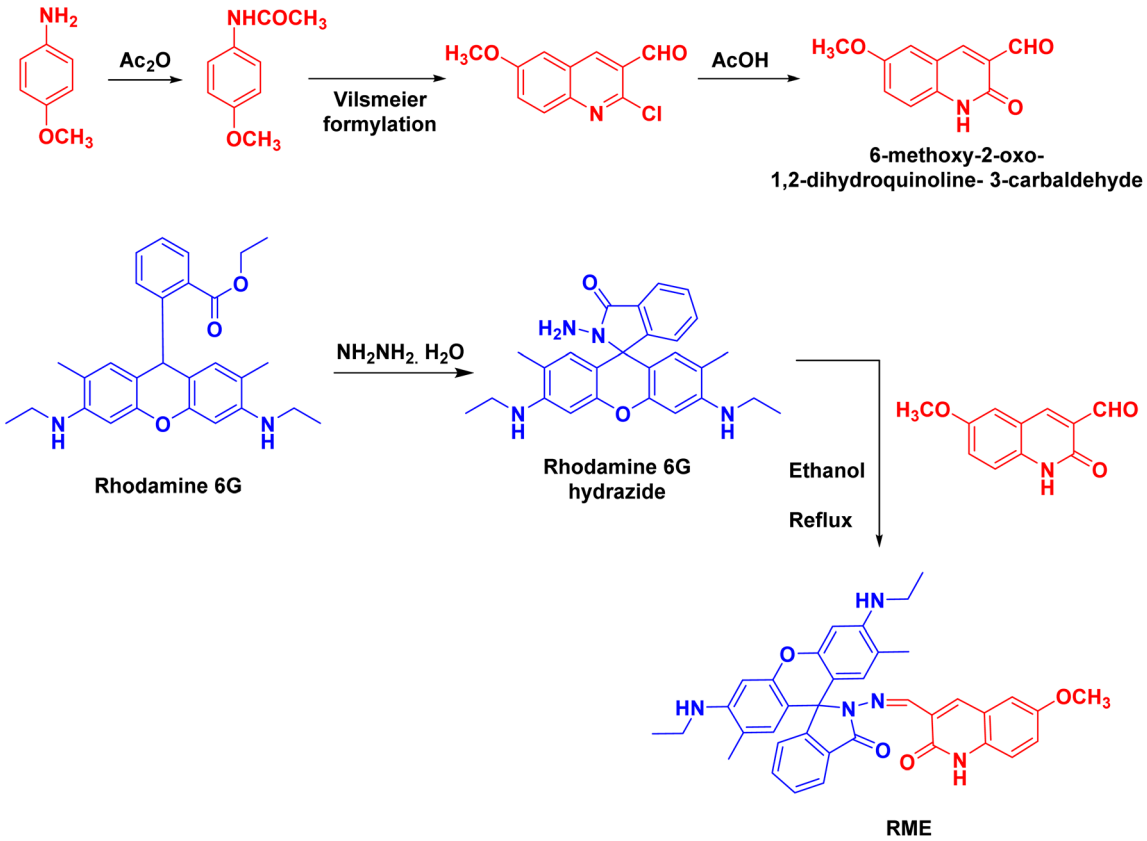

Scheme 1 Schematic representation for the synthesis of probe RME.

3.2. Spectrophotometric features of ratiometric/colorimetric selectivity of the receptor RME

UV-vis absorption spectrum investigations were performed to track the photophysical action of **RME** beforehand and following the different additions of Cu^{2+} ions. The related results are shown in Fig. 1a. In the absence of Cu^{2+} ions, the receptor **RME** shows three absorbance bands at 306 nm, 337 nm, and 410 nm, respectively, in the DMF/water medium (1 : 2, v/v) medium, which corresponds to the π–π* and n–π* transitions, respectively.[47] It can be seen from Fig. 3 that after the addition of Cu^{2+} ions to the receptor **RME**, the peak at 306 nm starts decreasing and the peak around 337 nm starts increasing; simultaneously there is a new absorption peak emerging at 525 nm in the visible region. **RME** with Cu^{2+} ions has a significant color change from yellow to pink. As a result, a noticeable color variation from yellow to pink is visible to the naked eye. It is evident that the addition of additional competing anions and cations (Mg^{2+}, Na^{+}, Zn^{2+}, Ni^{2+}, Ce^{3+}, Cd^{2+}, Bi^{2+}, K^{+}, Co^{2+}, Ca^{2+}, Fe^{2+}, Fe^{3+}, HSO^{3-}, Ag^{+}, Pb^{2+}, Cl^{-}, Br^{-}, Ba^{2+}, I^{-}, NO^{3-}, and Cr^{3+}) to the appropriate medium (**RME**) does not affect the color or spectral features of the **RME** receptor (inset of Fig. 1b). Additionally, ratiometric (A_{525}/A_{410}) investigation for Cu^{2+} may be accomplished utilizing these two wavelengths; other interfering anions and cations including Mg^{2+}, Na^{+}, Zn^{2+}, Ni^{2+}, Cu^{2+}, Ce^{3+}, Cd^{2+}, Bi^{2+}, K^{+}, Co^{2+}, Ca^{2+}, Fe^{2+}, Fe^{3+}, HSO^{3-}, Ag^{+}, Pb^{2+}, Cl^{-}, Br^{-}, Ba^{2+}, I^{-}, NO^{3-}, and Cr^{3+} lack this capability, making **RME**-based ratiometric/colorimetric chemosensors extremely specific for Cu^{2+} ions (Fig. 1b).

3.3. Spectrophotometric titration experiments for RME with Cu^{2+} ions

At the same time, absorbance spectral changes of **RME** with incremental amounts of Cu^{2+} ions were monitored in DMF/water (1 : 2, v/v) medium, and the typical equilibrium process is depicted in Fig. 2. After measuring the spectra, it was discovered that the isosbestic point was in the 442 nm region, signifying the beginning of the formation of a stable complex between the Cu^{2+} ions and the receptor **RME** where the continuous addition of Cu^{2+} towards the receptor manifests a clear color shift, and the translucent solution turns pink. This event unequivocally demonstrates that Cu^{2+} binding causes the **RME** ring-opening structure. The notable spectral changes, colorimetric alterations, and a new absorbance peak that appeared at 525 nm should be attributed to the characteristic peak for the Cu^{2+} ion induced by the open ring-closed spirolactam ring in the receptor **RME**.[48] According to colorimetric measurements, the aforementioned findings show that the receptor **RME** recognizes Cu^{2+} ions highly preferentially. To calculate the lowest limit of detection (LOD) of the ratiometric detection tactic, the calibration curve was plotted between the (A_{525}/A_{410}) and the different concentrations of Cu^{2+} ions. In the concentration range of 10 μM to 100 μM, good linear behavior was attained with a correlation coefficient of 0.99. The LOD was

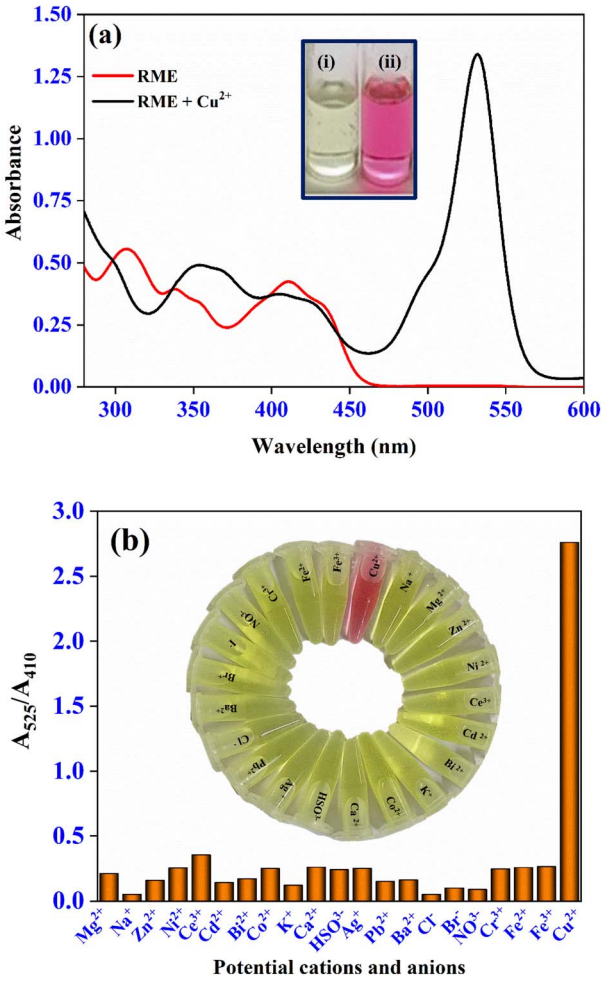

Fig. 1 UV-vis absorption spectral profile (a) for RME (10 μM) and after the addition of Cu^{2+} ions (100 μM) and the inset represents the RMEbefore (i) and after (ii) the addition of Cu^{2+} ions into the receptor RME in DMF/water (1 : 2, v/v) medium. Bar graph (b) of RME with the addition of different metal cations and anions and the inset visualizes the notable color changes of RME solution containing different metal cations and anions in DMF/water (1 : 2, v/v) medium.

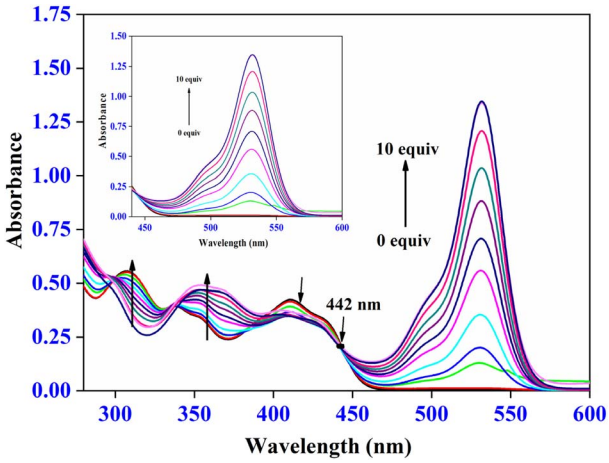

Fig. 2 UV-visible absorption spectra of RME (10 μM) upon adding Cu^{2+} ions (0–100 μM) into DMF/aqueous (1 : 2, v/v) medium and the inset shows the magnified view of the newly appeared peak at 525 nm.

estimated to be 11.25 nM by using the formula LOD = $3\sigma/S$, σ is the standard deviation of five measurements taken in the blank (0.0015) and S shows the calibration curve's slope (Fig. S5†). The determined LOD is significantly less than the maximum allowable level of Cu^{2+} ions in drinking water that has been approved by the WHO.

3.4. Fluorescence emission spectroscopic studies of receptor RME with Cu^{2+} ions

To further verify the binding ability of **RME** with Cu^{2+} ions, emission spectral studies were carried out. The fluorescence emission titration experiment was carried out with the incremental addition of Cu^{2+} ions to the receptor **RME** in DMF–H_2O (1 : 2, v/v). Upon the addition of Cu^{2+} ions to the receptor **RME**, the emission intensity (550 nm) starts to gradually increase (approx. 14-fold) (Fig. 3) with a strong red shift in the wavelength. Due to the fluorescence resonance energy transfer (FRET) method, the probe RME showed a rise in fluorescence in the DMF/water medium when stimulated at 415 nm as the concentration of Cu^{2+} increased.[49] Under an UV lamp, when Cu^{2+} was added to the **RME** chemosensor, no notable color change was noticed. The paramagnetic couple Cu^{2+} interact in many ways would make sense if the resultant strong fluorescent complex between **RME** and Cu^{2+} ions. This strong interaction could induce the spirolactam ring of (**RME**) and subsequently increase the fluorescence of the xanthenyl moiety.[50] Based on the emission enhancement, the concentrations of Cu^{2+} ions were quantified. Then, the LOD value was determined by using the equation, LOD = $3\sigma/S$, which was applied to calculate the limit of detection (LOD) of **RME** for Cu^{2+} ions, which is defined as a signal-to-noise ratio (S/N) of 3.[51–53] From the calibration plot, the LOD value was calculated to be 1.42 nM, which is much lower than the WHO criteria (2 ppm). Therefore, the proposed work is more appropriate for the detection of Cu^{2+} ions in drinking water using the **RME** receptor. Furthermore, the effect of pH on **RME** and **RME** with Cu^{2+} ions was investigated by emission spectral

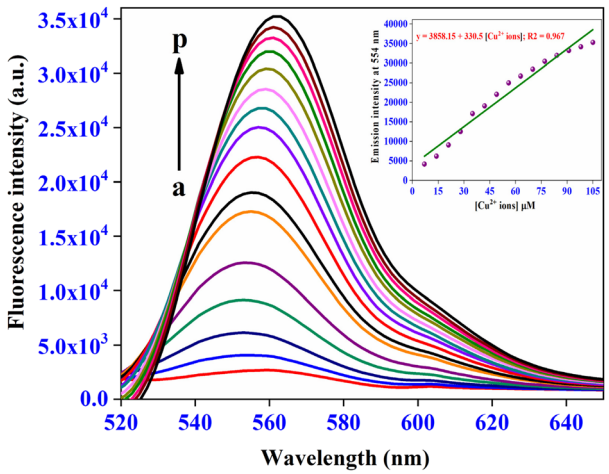

Fig. 3 Fluorescence spectra of RME solutions in the presence of Cu^{2+} ions in DMF/aqueous (1 : 2, v/v) medium.

studies. A pH of 4–10 was accomplished by mixing NaOH or HCl with 0.01 M phosphate buffer saline (PBS). The developed receptor **RME** and **RME** with Cu^{2+} ions display the maximum emission intensity in neutral pH around 6 to 8 (Fig. S6†). Thus, we have kept the pH at 7 for all sensing experiments.

3.5. Density functional theory calculations

A molecular-level investigation was conducted into the process of complex formation between the **RME** and Cu^{2+} ions using a density functional theory-based computational technique which was optimized at the B3LYP/M06-2X functional and LANL2DZ basis set and the quantum chemical calculations were done using the Gaussian 16 software package. The Cu^{2+} complex of **RME**, together with its optimal geometry and highest occupied molecular orbitals (HOMO) and lowest unoccupied molecular orbitals (LUMO), is displayed in Fig. 4. It is evidenced from Fig. 4 that the HOMO was dispersed across the rhodamine core and the LUMO was dispersed in the quinoline moiety. After the coordination of **RME** with Cu^{2+} ions, the HOMO and LUMO were dispersed in the rhodamine core.

The DFT-optimized structures of the receptor **RME** and RME–Cu^{2+} ensemble are disclosed in Fig. S7.† From Fig. S7,† the geometry of RME–Cu^{2+} is trigonal bipyramidal, where the receptor **RME** coordinates with Cu^{2+} through quinoline (–C=O), imine (–CH=N) and ring-opened (–C–O) with calculated bond distances of 2.001 Å, 1.998 Å and 2.029 Å respectively (Fig. S7†). The SO_4^{2-} formed a coordination with Cu^{2+} with bond distances of 2.413 Å and 1.979 Å respectively. The HOMO–LUMO energy level gap for the complex is 4.437 eV, while the energy level gap for the HOMO and LUMO of the probe **RME** is 5.528 eV. Based on the previously described results, the RME–Cu^{2+} complex showed a smaller frontier orbital gap than the receptor **RME**, which made it more reactive and polarizable.

3.6. Reversibility experiments with RME and EDTA

Reversibility research is crucial for the growth of chemo biosensors with high degrees of specificity and sensitivity for components required for accurate and efficient analyte detection in real-world applications. Using EDTA, a chelating agent, as a coordinating receptor to ascertain the probe's reusable feature in the absorbance detection process allowed for the determination of the probe RME's reversibility towards Cu^{2+} ions. The Cu^{2+} analyte and the probe **RME** were first coupled experimentally to generate a complex at 550 nm in DMF–H_2O (1 : 1, v/v).

After adding EDTA, the RME–Cu^{2+} complex was found to have returned to its original state (Scheme 2). When the EDTA–Cu^{2+} complex formed, the pink hue of the RME–Cu^{2+} complex returned to the pale-yellow color of the free receptor **RME**. A series of investigations were conducted to test the receptor reversibility, and the results established that the probe can

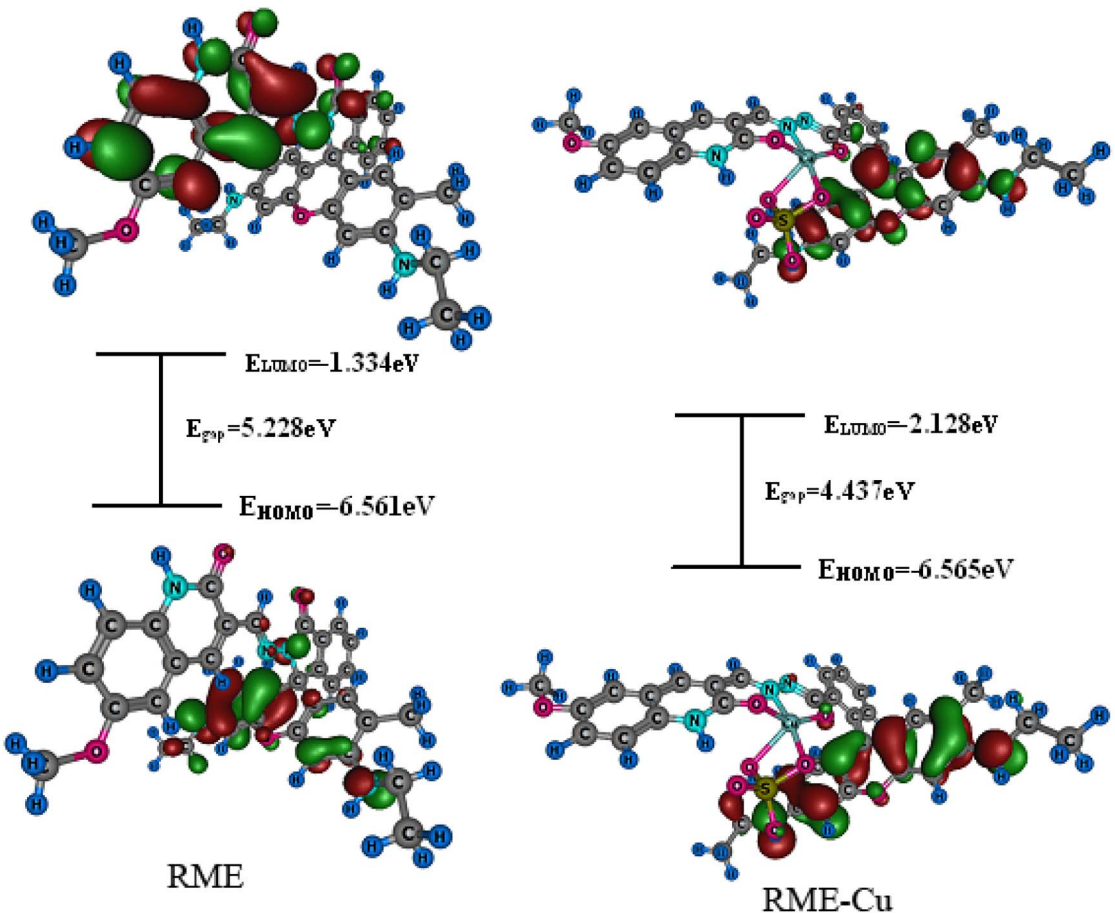

Fig. 4 Frontier molecular orbital energy levels of the RME–Cu^{2+} complex calculated using the B3LYP/M06-2X functional and LANL2DZ basis set.

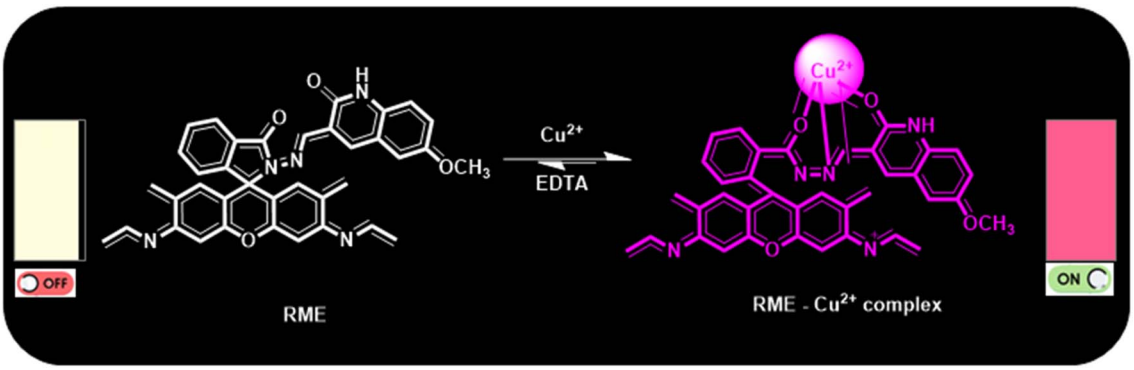

Scheme 2 Plausible mechanism for the formation of the RME–Cu^{2+} complex and reversibility with a chelating agent, EDTA.

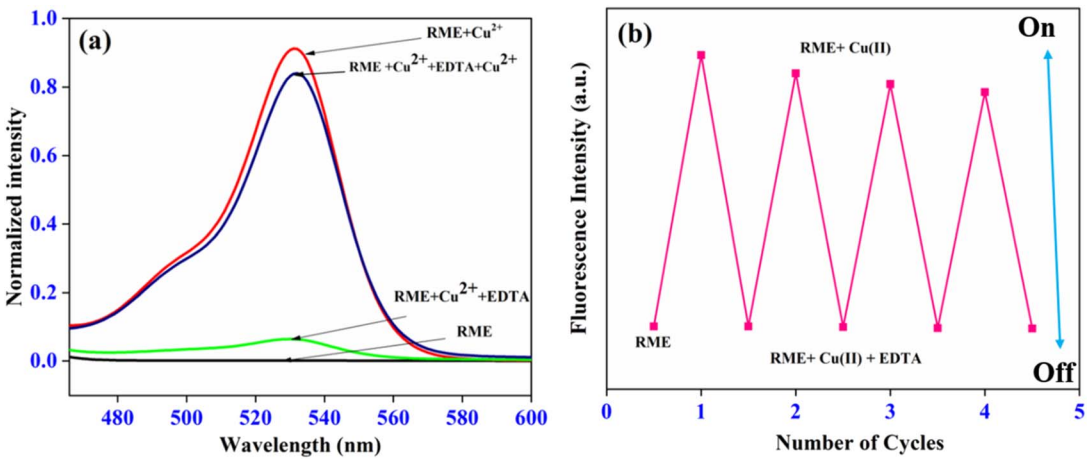

Fig. 5 Reversibility spectra (a) and cycle (b) of **RME** towards Cu^{2+} (100 μM) along with EDTA (100 μM).

detect Cu^{2+} ions four times, as shown in (Fig. 5a and b). This reaction has shown a decrease in emission intensity when the Cu^{2+} ions are added to the RME + Cu^{2+} ions + EDTA combination. Nearly ~80% of the emission intensity was stored at the end of the fourth cycle (Fig. 5b). This investigation was conducted to evaluate the sensor's regularity and dependability in identifying certain analytes. Thus, it has been demonstrated that adding an EDTA solution can reverse the RME's reaction to the Cu^{2+} ion. The receptor **RME** is reusable because this cycle can potentially be repeated at least four times.

3.7. Logic gate behavior

Using the sequence-dependent fluorescence output between EDTA and Cu^{2+} ions as chemical inputs, we have studied the fluorescence "turn on" process of the probe **RME** to build the molecular logic gate behavior of the current system.[44,45] In this instance, an INHIBIT logic gate behavior corresponds quite well with this receptor **RME**. The given scenario uses the INHIBIT logic gate belongings of the probe **RME**, Cu^{2+} ions, and EDTA as inputs (1 & 2) and the fluorescence peak intensity at 525 nm as the output (Fig. 6a). The logic gate is ON if the output is "1", and this behavior can only be seen when Cu^{2+} ions are present. In three distinct scenarios, the existence of EDTA, the occurrence of both EDTA and Cu^{2+} ions, and without mixing of both EDTA and Cu^{2+} ions if the output is "0", it indicates that the logic gate is OFF. These results implied that the behavior of the receptor **RME** is that of an INHIBIT logic gate.[45] There are probably several interactions between the paramagnetic Cu^{2+} ions, which results in the production of a highly fluorescent complex with RME. The spirolactam ring in RME may open as a result of this interaction, increasing the fluorescence of the xanthenyl moiety. The INHIBIT logic gate was the subject of another logic gate application carried out for the study (Fig. 6b–d). Herein, Cu^{2+} and EDTA signify input values 1 and 2, while color change (Fig. 6b), and/or A_{525}/A_{410} (Fig. 6c), the outputs. In these systems, when both inputs are absent (0, 0), both inputs are present (1, 1), or input 2 is present but input 1 is absent (0, 1), the output of these systems is 0. In contrast, the result is 1 when input 1 is present and input 2 is not (1, 0) (Fig. 6d). This action, which results in a color shift from yellow to pink, is explained by the Cu^{2+} ions producing an enhanced absorbance band that is dependent on the concentration at 525 nm.

3.8. Paper strip based applications

Because they are inexpensive to prepare, paper-strip-based chemosensors can be used in a wide range of settings, including those with limited resources and on-site monitoring applications. Numerous chemosensors based on paper offer prompt

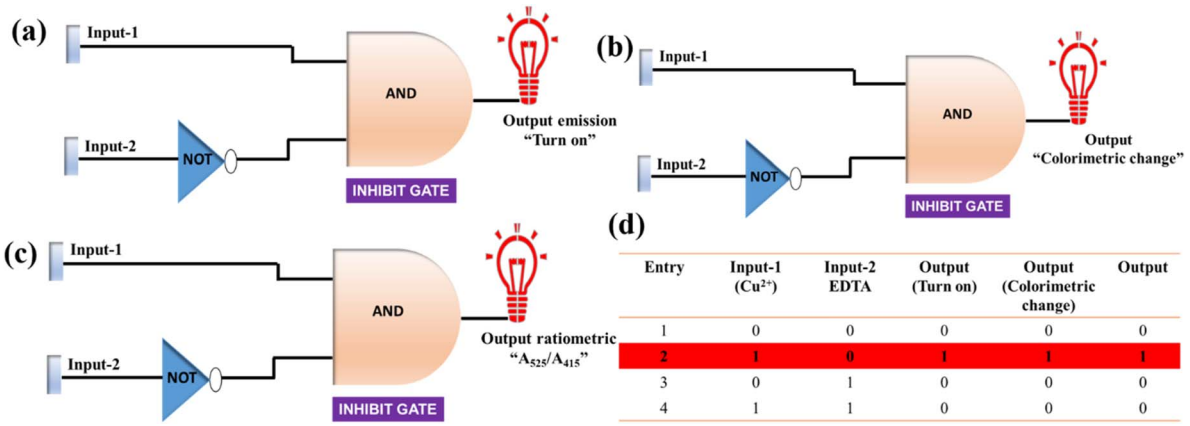

Entry	Input-1 (Cu^{2+})	Input-2 EDTA	Output (Turn on)	Output (Colorimetric change)	Output
1	0	0	0	0	0
2	1	0	1	1	1
3	0	1	0	0	0
4	1	1	0	0	0

Fig. 6 (a) Construction of the truth table of the IMPLICATION logic circuit for output as emission turn on (b), output as colorimetric change (c), output as ratiometric features A_{525}/A_{410}, and the truth table (d). Truth table representation for the IMPLICATION logic gate.

data, enabling prompt executive processing. For instance, certain organic molecules can yield outcomes in a couple of minutes, which is crucial in situations like ecological tracking or food-related investigations where speed is of the essence. In this work, Whatman filter paper was soaked in an **RME**-dissolved DMF/water mixture to develop paper-based sensor test strips which contain 2.5 mL of the receptor **RME** dissolved DMF/water mixture, and kept soaked for more than 5 min. Before applying the Cu^{2+} ion sensor, the paper-based test strips were allowed to air dry for almost eight hours. **RME**-deposited paper strips with incremental quantities of Cu^{2+} ions were investigated and the corresponding colorimetric photographs are illustrated in Fig. 7. Before the spiking of Cu^{2+} ions, paper strips were slight yellow in color. As the concentration of metal ions increased, the test strip's pink color got more vibrant, and as illustrated in Fig. 7, it was able to detect Cu^{2+} at concentrations as low as 20 μM using receptor **RME**. Additionally, the RME–Cu^{2+} complex has been applied as an organic ink. Initially, Whatman filter paper was dipped in the receptor **RME** (100 μM) for 5 min and then it was dried under air. This paper is yellow in color. Subsequently, a butterfly was sketched and inscribed using Cu^{2+} ions (50 μM) on the **RME**-coated paper strips; both the written word and the butterfly are readily visible to the naked eye. These findings demonstrate that the RME–Cu^{2+} complex was applied for (ink or marker) writing purposes on the filter paper.

3.9. Integration of the smartphone with the present colorimetric method

A straightforward facile to use smartphone testing may additionally validate the color variation for **RME** in the presence of Cu^{2+} ions in DMF/water medium, as it yields more accurate and sensitive results than optical detection. Here, the various quantities of Cu^{2+} ions are mixed distinctly with the standard solution of the probe **RME** (100 μM) in DMF/water medium and the corresponding color variation photograph is illustrated in the inset of Fig. 8. An existing smartphone color app (color picker) was used to resolve the red, green, and blue (RGB) primary color intensity values. This smartphone-based sensing

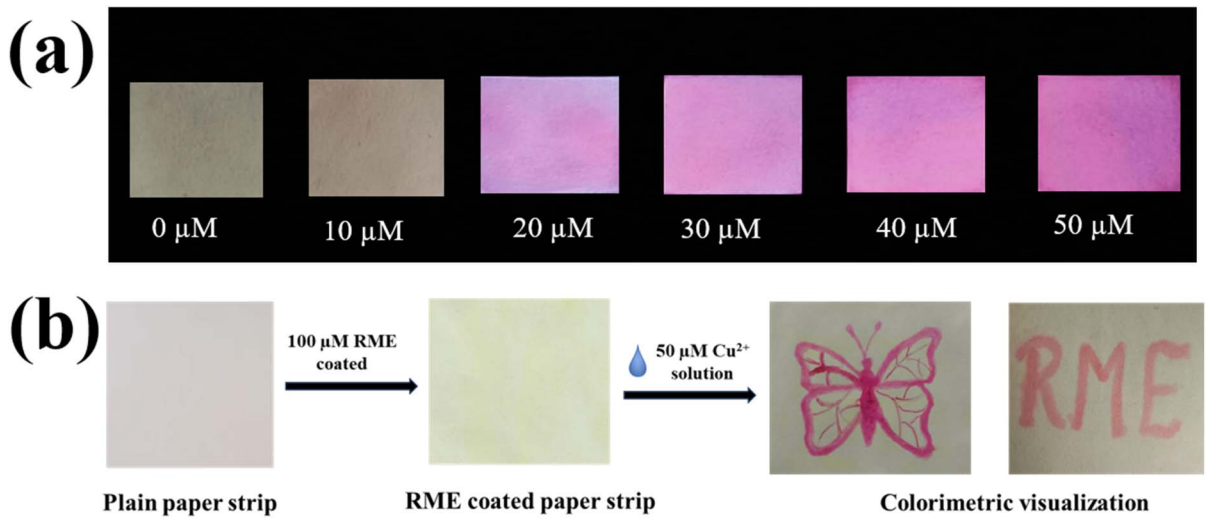

Fig. 7 (a) Colour changes of the RME sensor filter paper test strips with the increasing concentration of the Cu^{2+} solution. (b) Colour changes observed upon the addition of Cu^{2+} in the stock solution of the RME-soaked paper strip.

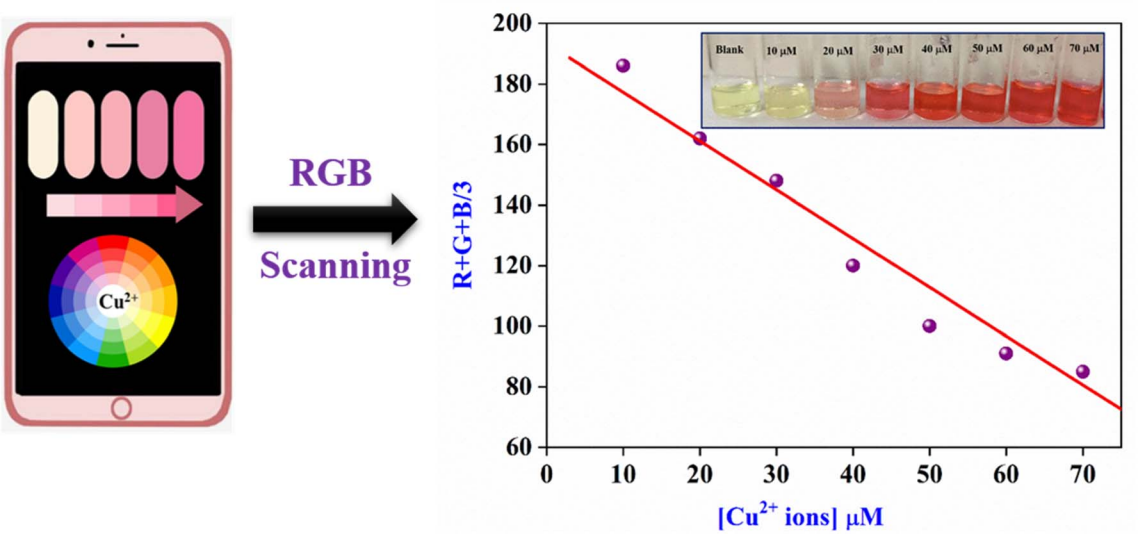

Fig. 8 The calibration curve of the RGB color response using a smartphone and the inset shows a color variance of **RME** with different amounts of Cu^{2+} ions in DMF/aqueous (1 : 2, v/v) medium.

technique primarily interprets digital photos of glass vials containing colloidal solutions using RGB values, which cover from 0 to 255. These systems are capable of translating color into RGB values using values like [0, 0, 0] for pure black and [255, 255, 255] for white.[53] Descriptive photos of each set of the probe **RME** solution with varying concentrations of Cu^{2+} ions were taken using the smartphone. By keeping a constant distance from the smartphone, the receptor **RME** with and without Cu^{2+} ion solutions was captured in a picture against a white background. The receptor **RME** solution's color gradually changed from slightly yellow to pink as the concentration of Cu^{2+} ions raised from 10 to 70 μM. The mean RGB values and Cu^{2+} ion concentrations between 10 and 70 μM were regressed linearly using the equation $y = 193.35 + 1.61$ [Cu^{2+} ions] with $R^2 = 0.978$. A calibration curve can be constructed using the average RGB value's linear increase with the quantities of Cu^{2+} ions as displayed in Fig. 8. From the slope of the linear calibration curve, the value of LOD is calculated to be 107 nM, which is quite lower than the tolerable limits by authorities' reports. As a result, a quick, easy, on-site, and reasonably priced method of detecting Cu^{2+} ions based on the receptor RME's color fluctuation is made possible *via* smartphone applications. Table S1† summarizes the collected analytical parameters of the current approach and compares them with those of previously published methods of Cu^{2+} ion detection using relevant chemical compounds. Table S1† illustrates the three distinct methods for detecting Cu^{2+} ions, which can be two to three orders extended or have comparable LOD values. It may contribute to the **RME** sensing probe's excellent qualities, such as its quick reaction time, lowest detection limit, selectivity, and so forth (**RME**).

3.10. Selectivity of RME towards various metal ions

Selectivity is a crucial factor for the chemosensors. The fluorescence selectivity experiments of the synthesized receptor, **RME** towards potentially interfering metal cations anions including Mg^{2+}, Na^{+}, Zn^{2+}, Ni^{2+}, Cu^{2+}, Ce^{3+}, Cd^{2+}, Bi^{2+}, K^{+}, Co^{2+}, Ca^{2+}, Co^{2+}, HSO^{3-}, Ag^{+}, Pb^{2+}, Cl^{-}, Br^{-}, Ba^{2+}, I^{-}, NO^{3-}, Cr^{3+} and Cu^{2+} were tracked in DMF–H_2O (1 : 1, v/v) medium and the results are outlined in Fig. 9. As evidenced from Fig. 9, with the addition of 5-fold increasing amounts of different metal ions to the **RME** solution, only the Cu^{2+} ions induced a complete fluorescence enhancement of the receptor, **RME** (Fig. 9). The other abovementioned metal cations and anions such as Mg^{2+}, Na^{+}, Zn^{2+}, Ni^{2+}, Cu^{2+}, Ce^{3+}, Cd^{2+}, Bi^{2+}, K^{+}, Co^{2+}, Ca^{2+}, Co^{2+}, HSO^{3-}, Ag^{+}, Pb^{2+}, Cl^{-}, Br^{-}, Ba^{2+}, I^{-}, NO^{3-}, and Cr^{3+} could not induce any change in the emission intensity and colorimetric nature under daylight. These findings suggested that the receptor **RME** might function as a colorimetric and fluorescence chemosensor that is selective for Cu^{2+} ions. To understand the binding nature of Cu^{2+} with **RME**, the continuous variation method (Job's plot) was applied, in which the intensity of the band was plotted against the molar fraction of **RME** (Fig. S8†). The observed results suggested the formation of 1 : 1 stoichiometry between **RME** and Cu^{2+} during their complexation. Furthermore, the 1 : 1 binding stoichiometry was confirmed through the mass spectroscopy *m*/*z* value of 774.34 (Fig. S9†).

3.11. Practical applications

The amounts of Cu^{2+} ions in tap, dam, and drinking water samples were successfully measured using the probe **RME**. To find the Cu^{2+} ions in actual water samples, a conventional addition technique was used.[52] In the drinking, dam, and tap water samples, Cu^{2+} ions were first not found. To account for a notable rise in emission intensity for triplicate observations, Cu^{2+} ions were mixed into environmental water samples. Table S2† displays the actual water research observations that were gathered. When Cu^{2+} ions were introduced into tap, dam, and drinking water samples, there was an outstanding recovery from 91.75 to 96.82%. The current method's great accuracy was

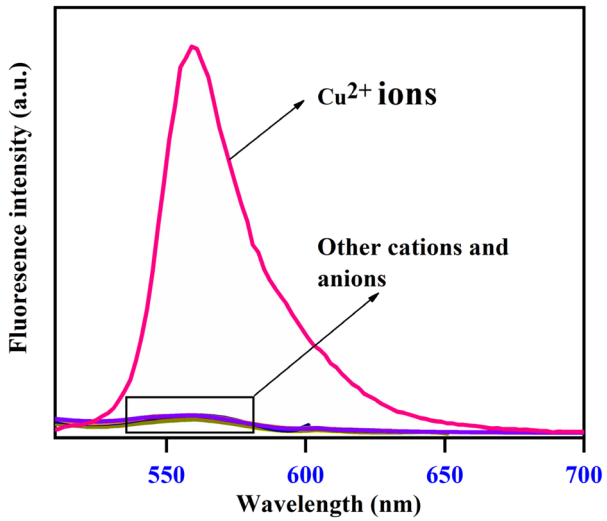

Fig. 9 Fluorescence spectra of **RME** with different metal cations and anions including Mg^{2+}, Na^{+}, Zn^{2+}, Ni^{2+}, Cu^{2+}, Ce^{3+}, Cd^{2+}, Bi^{2+}, K^{+}, Co^{2+}, Ca^{2+}, Co^{2+}, HSO^{3-}, Ag^{+}, Pb^{2+}, Cl^{-}, Br^{-}, Ba^{2+}, I^{-}, NO^{3}, Cr^{3+} and Cu^{2+} in DMF/H_2O (1 : 2, v/v) medium.

suggested by its lowest relative standard deviation value (>2.21%).

4. Conclusion

In conclusion, a new rhodamine and quinoline-based simple naked eye and switch-on luminescent receptor (**RME**) has been efficaciously synthesized for Cu^{2+} ion recognition in DMF/water (1 : 2, v/v) medium. The spirolactam compound demonstrated outstanding specificity towards Cu^{2+} ions over other typically occurring cations in conventional DMF/H_2O medium. Upon the interaction of Cu^{2+} ions, the receptor color varied from slightly yellow to pink in color which was easily viewed by the naked eye whereas strong spectral fluctuations were noticed in absorbance and emission studies. **RME** showed a good sensing performance for Cu^{2+} ions with LOD 11.25 nM for ratiometric colorimetry, 1.42 nM for fluorometry, and 107 nM for the smartphone-based detection strategy, significantly lower than the tolerable limits (20 μM) by WHO. The mass spectral analysis, Job's plot, and DFT method were employed to reveal the probable 1 : 1 stoichiometric complexation mode between Cu^{2+} ions and the receptor **RME**. Furthermore, the developed fluorescence sensor was applied for the detection of Cu^{2+} ions in environmental water samples such as tap, dam, and drinking water samples. Additionally, practical smartphone and paper-based test strip applications were utilized to fruitfully accomplish both qualitative and quantitative Cu^{2+} ion quantification, avoiding the need for sophisticated equipment and enabling accurate and reasonably priced on-site assessment of potential Cu^{2+} ions.

Data availability

The authors ensure that all the data mentioned in this paper are available on request.

Conflicts of interest

The authors declare no conflict of interest.

Acknowledgements

This research work has been supported financially by the Department of Science and Technology (DST/TDT/TC/RARE/2022/13) dated 27.03.2023. The author also acknowledges NMR facility, CIC, Bharathiar University supported by DST (PURSE Phase II programme), New Delhi. The authors would like to extend their sincere appreciation to the Researchers Supporting Project number (RSPD2025R694), King Saud University, Riyadh, Saudi Arabia.

References

1 M. R. Awual, I. M. M. Rahman, T. Yaita, M. A. Khaleque and M. Ferdows, pH dependent Cu(II) and Pd(II) ions detection and removal from aqueous media by an efficient mesoporous adsorbent, *Chem. Eng. J.*, 2014, **236**, 100–109.
2 E. Fan, H. Guo, T. Hao, R. Zhao, P. Zhang, Y. Feng, Y. Liu and K. Deng, Morpholine-modified polyacrylamides with polymerization-induced emission and its specific detection to Cu^{2+} ions, *Spectrochim. Acta, Part A*, 2024, **309**, 123782.
3 D. G. J. Barceloux, *Clin. Toxicol.*, 1999, **37**, 217.
4 V. Kumar, J. Kalita, H. K. Bora and U. K. Misra, Temporal kinetics of organ damage in copper toxicity: A histopathological correlation in rat model, *Regul. Toxicol. Pharmacol.*, 2016, **81**, 372–380.
5 M. S. Moorthy, H. J. Cho, E. J. Yu, Y. S. Jung and C. S. Ha, A modified mesoporous silica optical nanosensor for selective monitoring of multiple analytes in water, *Chem. Commun.*, 2013, **49**, 8758–8760.
6 R. Chandra, A. Ghorai and G. K. Patra, A simple benzildihydrazone derived colorimetric and fluorescent 'on–off–on' sensor for sequential detection of copper(II) and cyanide ions in aqueous solution, *Sens. Actuators, B*, 2018, **255**, 701–711.
7 H. S. Jung, M. Park, D. Y. Han, E. Kim, C. Lee, S. Ham and J. S. Kim, Cu^{2+} Ion-Induced Self-Assembly of Pyrenylquinoline with a Pyrenyl Excimer Formation, *Org. Lett.*, 2009, **11**, 3378–3381.
8 Y. Zhou, F. Wang, Y. Kim, S. J. Kim and J. Yoon, Cu^{2+}-Selective Ratiometric and "Off-On" Sensor Based on the Rhodamine Derivative Bearing Pyrene Group, *Org. Lett.*, 2009, **11**, 4442–4445.
9 M. S. Moorthy, M. J. Kim, J. H. Bae, S. S. Park, N. Saravanana, S. H. Kim and C. S. Ha, Multifunctional periodic mesoporous organosilicas for biomolecule recognition, biomedical applications in cancer therapy, and metal adsorption, *Eur. J. Inorg. Chem.*, 2013, **2013**, 3028–3038.
10 D. H. Joo, J. S. Mok, G. H. Bae, S. E. Oh, J. H. Kang and C. Kim, Colorimetric Detection of Cu^{2+} and Fluorescent Detection of PO_4^{3-} and S^{2-} by a Multifunctional Chemosensor, *Ind. Eng. Chem. Res.*, 2017, **56**, 8399–8407.

11 WHO, *Guidelines for Drinking-Water Quality*, World Health Organization (WHO), Geneva, 2011.
12 S. C. Chibueze Izah, N. Chakrabarty and A. L. Srivastsav, A Review on Heavy Metal Concentration in Potable Water Sources in Nigeria: Human Health Effects and Mitigating Measures, Expo, *Health*, 2016, **8**, 285–304.
13 M. S. Moorthy, H. B. Kim, A. R. Sung, J. H. Bae, S. H. Kim and C. S. Ha, Fluorescent mesoporous organosilicas for selective monitoring of Hg^{2+} and Fe^{3+} ions in water and living cells, *Microporous Mesoporous Mater.*, 2014, **194**, 219–228.
14 S. J. Kulkarni, Heavy metal pollution: sources, effects, and control methods, in *Hazardous Waste Management and Health Risks*, 2020, pp. 97–112.
15 A. Senthil Murugan, E. R. Abel Neolson and J. Annaraj, Solvent dependent colorimetric, ratiometric dual sensor for copper and fluoride ions: Real sample analysis, cytotoxicity and computational studies, *Inorg. Chim. Acta.*, 2016, **450**, 131–139.
16 G. Liao, C. Zheng, D. Xue, C. Fan, G. Liu and S. Pu, A diarylethene-based fluorescent chemosensor for the sequential recognition of Fe^{3+} and cysteine, *RSC Adv.*, 2016, **6**, 34748–34753.
17 L. Jin, C. Liu, N. An, Q. Zhang, J. Wang, L. Zhao and Y. Lu, Fluorescence turn-on detection of Fe^{3+} in pure water based on a cationic poly(perylene diimide) derivative, *RSC Adv.*, 2016, **6**, 58394–58400.
18 Y. S. Kim, J. J. Lee, S. Y. Lee, T. G. Jo and C. Kim, A highly sensitive benzimidazole-based chemosensor for the colorimetric detection of Fe(II) and Fe(III) and the fluorometric detection of Zn(II) in aqueous media, *RSC Adv.*, 2016, **6**, 61505–61515.
19 A. Luo, H. Wang, Y. Wang, Q. Huang and Q. Zhang, A novel colorimetric and turn-on fluorescent chemosensor for Iron(III) ion detection and its application to cellular imaging, *Spectrochim. Acta: Mol. Biomol. Spectrosc.*, 2016, **168**, 37–44.
20 M. Mirzaei, M. Behzadi, N. M. Abadi and A. Beizaei, Simultaneous separation/preconcentration of ultra-trace heavy metals in industrial wastewaters by dispersive liquid–liquid microextraction based on solidification of floating organic drop prior to determination by graphite furnace atomic absorption spectrometry, *J. Hazard Mater.*, 2011, **186**, 1739–1743.
21 R. Sitko, P. Janik, B. Zawisza, E. Talik, E. Margui and I. Queralt, Green Approach for Ultratrace Determination of Divalent Metal Ions and Arsenic Species Using Total-Reflection X-ray Fluorescence Spectrometry and Mercapto-Modified Graphene Oxide Nanosheets as a Novel Adsorbent, *Anal. Chem.*, 2015, **87**(6), 3535–3542.
22 M. S. Moorthy, Y. Oh, S. Bharathiraja, P. Manivasagan, T. Rajarathinam, B. Jang, T. T. V. Phan, H. Jang and J. Oh, Synthesis of amine-polyglycidol functionalised Fe_3O_4@SiO_2 nanocomposites for magnetic hyperthermia, pH-responsive drug delivery, and bioimaging applications, *RSC Adv.*, 2016, **6**, 110444–110453.
23 S. Petrović, V. Guzsvány, N. Ranković, J. Beljin, S. Rončević, B. Dalmacija, A. M. Ashrafi, Z. Kónya, I. Švancara and K. Vytřas, Trace level voltammetric determination of Zn(II) in selected nutrition related samples by bismuth-oxychloride-multiwalled carbon nanotube composite based electrode, *Microchem. J.*, 2019, **146**, 179–186.
24 I. P. Oliveri, G. Munzi and S. D. Bella, A simple approach based on transmetalation for the selective and sensitive colorimetric/fluorometric detection of copper(II) ions in drinking water, *New J. Chem.*, 2022, **46**, 18018–18024.
25 M. S. Moorthy, H. J. Song, J. H. bae, S. H. Kim and C. S. Ha, Red fluorescent hybrid mesoporous organosilicas for simultaneous cell imaging and anticancer drug delivery, *RSC Adv.*, 2014, **4**, 43342–43345.
26 G. Sivaraman, V. Sathiyaraja and D. Chellappa, Turn-on fluorogenic and chromogenic detection of Fe(III) and its application in living cell imaging, *J. Lumin.*, 2014, **145**, 480–485.
27 S. Shyamsivappan, A. Saravanan, N. Vandana, T. Suresh, S. Suresh, R. Nandhakumar and P. S. Mohan, Novel quinoline-based thiazole derivatives for selective detection of Fe^{3+}, Fe^{2+}, and Cu^{2+} ions, *ACS Omega*, 2020, **42**, 27245–27253.
28 M. E. Germain and M. J. Knapp, Optical explosives detection: from color changes to fluorescence turn-on, *Chem. Soc. Rev.*, 2009, **28**, 2543–2555.
29 K. Saravana Mani, R. Rajamanikandan, B. Murugesapandian, R. Shankar, G. Sivaraman, M. Ilanchelian and S. P. Rajendran, Coumarin based hydrazone as an ICT-based fluorescence chemosensor for the detection of Cu^{2+} ions and the application in HeLa cells, *Spectrochim. Acta, Part A*, 2019, **214**, 170–176.
30 J. R. Lakowicz, *Principles of Fluorescence Spectroscopy*, Kluwer Academic, New York, 1999.
31 M. Santhamoorthy, K. Thirupathi, T. Periyasamy, D. Thirumalai, V. Ramkumar and S. C. Kim, Ethidium bromide-bridged mesoporous silica hybrid nanocarriers for fluorescence cell imaging and drug delivery applications, *New J. Chem.*, 2021, **45**, 20641–20648.
32 M. Shellaiah, P. Venkatesan, N. Thirumalaivasan, S. P. Wu and K. W. Sun, Pyrene-Based Fluorescent Probe for "Off-on-Off" Sequential Detection of Cu^{2+} and CN^- with HeLa Cells Imaging, *Chemosensors*, 2023, **11**(2), 115.
33 H. F. Xie, C. J. Yu, Y. L. Huang, H. Xu, Q. L. Zhang, X. H. Sun, X. Feng and C. Redshaw, A turn-off fluorescent probe for the detection of Cu^{2+} based on a tetraphenylethylene-functionalized salicylaldehyde Schiff-base, *Mater. Chem. Front.*, 2020, **4**, 1500–1506.
34 T. Simon, M. Shellaiah, V. Srinavasadesikan, C. C. Lin, F. H. Ka, K. W. Sun and M. C. Lin, Novel anthracene- and pyridine-containing Schiff base probe for selective "off–on" fluorescent determination of Cu^{2+} ions towards live cell application, *New J. Chem.*, 2016, **40**, 61010–6108.
35 S. K. Mishra, S. Dehuri and B. Bag, Effect of n-alkyl substitution on Cu(II)-selective chemosensing of rhodamine B derivatives, *Org. Biomol. Chem.*, 2020, **18**, 316–332.
36 R. Manjunath and P. Kannan, Highly selective rhodamine-based fluorescence turn-on chemosensor for Al^{3+} ion, *Opt. Mater.*, 2018, **79**, 38–44.

37 A. Pipattanawarothai and T. Trakulsujaritchok, Hybrid polymeric chemosensor bearing rhodamine derivative prepared by sol-gel technique for selective detection of Fe^{3+} ion, *Dyes Pigments*, 2020, **173**, 107946.
38 L. L. Chang, Q. Gao, S. Liu, C. C. Hu, W. J. Zhou and M. M. Zheng, Selective and differential detection of Hg^{2+} and Cu^{2+} with use of a single rhodamine hydrazone-type probe in the absence and presence of UV irradiation, *Dyes Pigments*, 2018, **153**, 117–124.
39 M. Iniya, D. Jeyanthi, K. Krishnaveni and D. Chellappa, Vitamin B_6 cofactor based fluorescent probe for sensing an anion (F^-) and cation (Co^{2+}) independently in a pure aqueous medium, *RSC Adv.*, 2014, **4**, 25393–35397.
40 V. Dujols, F. Ford and A. W. Czarnik, A Long-Wavelength Fluorescent Chemodosimeter Selective for Cu(II) Ion in Water, *J. Am. Chem. Soc.*, 1997, **119**(31), 7386–7387.
41 W. Breuer, S. Epsztejn, P. Millgram and I. Z. Cabantchik, Transport of iron and other transition metals into cells as revealed by a fluorescent probe, *Am. J. Physiol.: Cell Physiol.*, 1995, **268**, 1354–1361.
42 K. A. McCall and C. A. Fierke, Colorimetric and Fluorimetric Assays to Quantitate Micromolar Concentrations of Transition Metals, *Anal. Biochem.*, 2000, **284**(2), 307–315.
43 P. C. Crooker, N. Garrido and G. A. Ahearn, Copper transport by lobster hepatopancreatic epithelial cells separated by centrifugal elutriation: measurements with the fluorescent dye Phen Green, *J. Exp. Biol.*, 2001, **204**, 1433.
44 A. Senthil Murgan, N. Vidhyalakshmi, U. Ramesh and J. Annaraj, *In vivo* bio-imaging studies of highly selective, sensitive rhodamine based fluorescent chemosensor for the detection of Cu^{2+}/Fe^{3+} ions, *Sens. Actuators, B*, 2018, **274**, 22–29.
45 S. Kaleeswaran, D. S. Prabakaran, M. Santhamoorthy, S. Ansar, M. A. Farah, R. Rajamanikandan and K. S. Mani, Novel quinoline-based chemosensor as specific fluorescence sensing of copper ions in cancer cells and for organelle-specific imaging application, *Inorg. Chim. Acta*, 2025, **575**, 122440.
46 X. Xie, M. Pan, L. Hong, K. Liu, J. Yang, S. Wang and S. Wang, An "Off–On" Rhodamine 6G Hydrazide-Based Output Platform for Fluorescence and Visual Dual-Mode Detection of Lead(II), *J. Agric. Food Chem.*, 2021, **69**, 7209–7217.
47 B. S. Chauhan, A. Rai, A. K. Sonkar, K. Tripathi, S. Upadhyay, L. Mishra and S. Srikrishna, Neuroprotective Activity of a Novel Synthetic Rhodamine-Based Hydrazone against Cu^{2+}-Induced Alzheimer's Disease in *Drosophila*, *ACS Chem. Neurosci.*, 2022, **13**(10), 1566–1579.
48 A. Senthil Murugan, M. Kiruthika, E. R. Abel Noelson, P. Yogapandi, G. Gnana Kumar and J. Annaraj, Fluorescent sensor for in-vivo bio-imaging, precise tracking of Fe^{3+} ions in Zebrafish embryos and visual measuring of Cu^{2+} ions in pico-molar level, *Arab. J. Chem.*, 2021, **14**(1), 102910.
49 Y. Wang, H. Q. Chang, W. N. Wu, W. B. Peng, Y. F. Yan, C. M. He, T. T. Chen, X. L. Zhao and Z. Q. Xu, Rhodamine 6G hydrazone bearing pyrrole unit: Ratiometric and selective fluorescent sensor for Cu^{2+} based on two different approaches, *Sens. Actuators, B*, 2016, **228**, 395–400.
50 X. Q. Xu, X. J. Mao, Y. Wang, W. N. Wu, P. D. Mao, X. L. Zhao, Y. C. Fan and H. J. Li, Rhodamine 6G hydrazone with coumarin unit: a novel single-molecule multianalyte (Cu^{2+} and Hg^{2+}) sensor at different pH value, *RSC Adv.*, 2017, **7**, 42312–42319.
51 K. Wechakorn, U. Eiamprasert, J. Masoongnoen, A. Tantipanjaporn, P. Surawatanawong, P. Kanjanasirirat, Y. Pewkliang, S. Borwornpinyo, P. Kongsaeree and C. Pitsanuwong, A highly sensitive and selective rhodamine-semicarbazide based fluorescent sensor for Cu^{2+} detection in real water samples and fluorescence bioimaging in HepG2 cells, *Talanta*, 2024, **270**, 125530.
52 K. S. Mani, R. Rajamanikandan, G. Ravikumar, B. Vijaya pandian, P. Kolandaivel, M. Ilanchelian and S. P. Rajendran, Highly Sensitive Coumarin–Pyrazolone Probe for the Detection of Cr^{3+} and the Application in Living Cells, *ACS Omega*, 2018, **3**(12), 17212–17219.
53 K. S. Mani, R. Rajamanikandan, M. Ilanchelian, N. Muralidharan, M. Jothi and S. P. Rajendran, Smart phone assisted quinoline-hemicyanine based fluorescent probe for the selective detection of glutathione and the application in living cells, *Spectrochim. Acta, Part A*, 2020, **243**, 118809.

